Constructing A New CHF Look-Up Table Based on the Domain Knowledge Informed Machine Learning Methodology

Yue Jin, Koroush Shirvan
Department of Nuclear Science & Engineering
Massachusetts Institute of Technology
77 Massachusetts Ave, Cambridge, MA 02139, USA
yuejin@mit.edu; kshirvan@mit.edu

Xingang Zhao
Nuclear Energy and Fuel Cycle Division
Oak Ridge National Laboratory
1 Bethel Valley Rd, Oak Ridge, TN 37830, USA
zhaox2@ornl.gov

ABSTRACT

Accurate prediction of CHF under various fluid flow conditions continues to be required for design, operation and safety analysis of light water reactor rod bundles. Due to the lack of in-depth physical understanding as well as limited high-resolution data in the micro-scale flow and heat transfer, the existing models feature a sub-optimal uncertainty band. In this study, driven by the prior domain knowledge information obtained, an improved CHF look-up table is developed through unified machine learning algorithms for the vertical flow conditions within tube and annulus geometry. The Groeneveld 2006 look-up table is used as the domain knowledge to train machine learning process against tube and annulus CHF data for both DNB and DO type. The new look-up table shows improved accuracy for conditions relevant to PWRs and BWRs. In addition, its domain knowledge informed nature ensures that a rationale prediction can be made, thus accounting for previous valuable information in the machine learning model training process.

KEYWORDS
Critical heat flux; Machine learning; Domain knowledge informed; Look-up table

1. INTRODUCTION

Despite the long-lasting and extensive research campaign focused on the phenomenon of critical heat flux (CHF) phenomenon in the field of thermal-fluid sciences for decades, our fundamental understanding as well as the existing prediction capabilities for accuracy CHF occurrence are still progressing. This is partially due to the fact that there are many complexed two-phase flow and heat transfer processes involved (type of fluids and/or heating methodology, fluid local velocity and temperature distribution, local vapor generation mechanisms and density, sub-scale two-phase flow interface behavior, micro-scale heating surface morphology, system mass flow rate and pressure, etc.) and the limited resolution can be achieved by both available measurement techniques and analytical methodology under high-temperature high-pressures conditions relevant to nuclear industry.

Depending on different flow conditions and heat transfer mechanisms, CHF can be further distinguished as the dryout (DO) type, corresponding to high quality and low mass flux, and departure from nucleate

boiling type (DNB), corresponding to high subcooling and high mass flux. As a result, many correlations and alternative methods have been developed for better prediction of this phenomenon. For example, the W-3 correlation developed at Westinghouse [1], series of CISE correlations developed and improved at MIT [1]; GEXL correlation developed by GE [1]; CHF look-up table methodology developed by Groeneveld et al., 2007 [2]; and three-field model by Zhao et al., 2003 [3]. In order to further improve the operating efficiency and safety margin of energy systems, more accurate CHF prediction models are desirable.

Along with the significant advances in modern computational science and optimization theory, machine learning (ML) based regression techniques are quickly drawing attentions and provide an alternative approach to conventional predictive tools. The ML approach has unique strength in tackling complicated and non-linear problems with quick convergence speed, which makes it very suitable for solving multi-scale and multi-physics engineering problems like the one encountered in two-phase flow mass and heat transfer. Recently, a number of researchers investigated the feasibility of applying the ML techniques in predicting key thermal-hydraulic and safety parameters in nuclear engineering including Kim. et al., 2021 [4] for narrow rectangular channel applications, Jin et al., 2021 [5] and Zhao et al., 2020 [6] for CHF model development based on domain knowledge informed ML in various geometries, Park et al., 2020 [7] for wall temperature prediction at CHF, as well as He and Lee, 2018 [8] for CHF table construction using support vector machine.

This paper summarizes the recent effort in developing a new LUT based on the unified domain knowledge informed machine learning (DKIML) model trained for predicting the CHF in upward flow systems of various geometries (tube and annulus). The Groeneveld 2006 CHF LUT [2] is used as the domain knowledge to guide the learning process. Then, two advanced regression methods: the deep feed-forward neural network (NN) and random forest (RF) are used to construct unified CHF models. Then, a new LUT is constructed in the same way as Groeneveld 2006 CHF LUT based on the ML models, which are validated by experimental data. Improved prediction performance is obtained for the new LUT. The developed ML LUT can be validated and implemented into existing numerical codes to further improve their prediction capability and robustness.

2. DESCRIPTION OF METHODOLOGY

The two advanced ML methods that will be applied and evaluated in the current study are the random decision forest (RF) and the feed-forward deep neural network (NN). This section will provide a brief introduction of the two methods and the domain knowledge informed ML.

2.1. Introduction of ML Methods for Regression

The random decision forest (RF) constructs a multitude of decision trees at training time. It is a fast and flexible tree-based ML technique that produces reliable results without engaging in cumbersome hyperparameter tuning. By randomly selecting observations and features via the bootstrap aggregation technique, multiple decision trees are built, and predictions from each tree are then averaged to derive the final output. For classification tasks, the output of the random forest is the class selected by most trees. For regression tasks, the mean or average prediction of the individual trees is returned. **Figure 1** shows the configuration of the RF structure.

The artificial neural networks were inspired by information processing and distributed communication nodes in biological systems. It is a collection of connected units or nodes called artificial neurons, which loosely model the neurons in a biological brain. An artificial neuron that receives a signal then processes it and can signal neurons connected to it. The "signal" at a connection is a real number, and the output of each neuron is computed by some non-linear function of the sum of its inputs and weights. Typically, neurons

are aggregated into layers. Signals travel from the first layer (the input layer), to the last layer (the output layer), possibly after traversing the layers multiple times. Weights for each neurons are updated after each training batch through backward propagation base on different gradient descent learning algorithms, such as the Stochastic Gradient Descent (SGD) or Adaptive Moment Estimation (ADAM). The training process is repeated for certain times (epochs) such that the errors (e.g., "mse", "logcosh", etc.) are adequately reduced. A sketch of the NN architecture can be found in **Figure 2**.

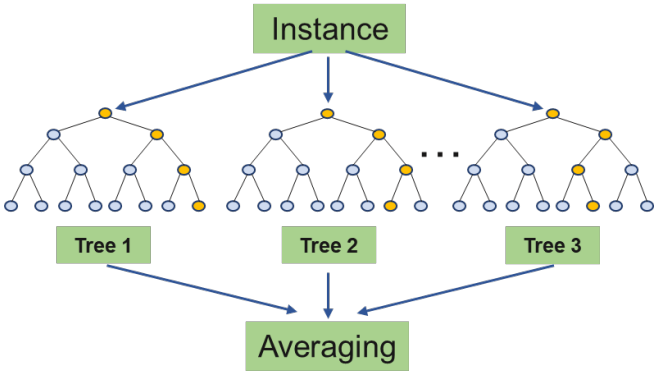

Figure 1. Sketch of Random Forest Method

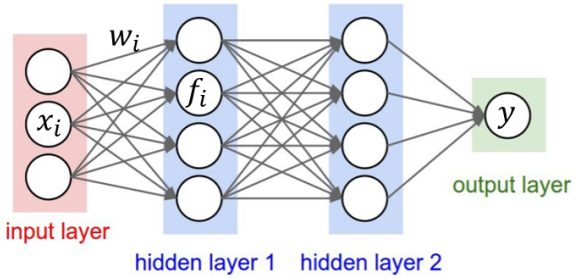

Figure 2. Sketch of Neuron Network Method

Both the above two regression methods allow for high generalization ability when properly sampled and trained. However, their training processes are generally unknown to the outside, which creates a so-called "black-box" problem.

2.2. Development of Domain Knowledge Informed Machine Learning Models

In order to solve this "black-box" problem, the DKIML method are introduced in the current work, as is shown in **Figure 3**. This method stems from the idea that already established and validated prior knowledge space information is valuable and can be used to assist the ML training process and reduce un-physical data scatter, since the prior knowledge, usually existed as correlations, models or formulated database, is capable of providing credible baseline solutions for the ML training process.

For DKIML, a conventional physics model, $f(x)$, is selected as the fixed-structure prior model providing baseline prediction, $\hat{y}_p$. ML is then used to learn from the residuals, ε, between true value, y, and the physics model predicted output, which would effectively minimize the ML training loss function. Input feature space, x, is available to both components of the prior and ML model, although their input features might be different. Once the DKIML model is trained, the final predicted CHF output, $\hat{y}_h$, can be obtained by adding the baseline prediction, $\hat{y}_p$, with ML predicted residual, $\hat{\varepsilon}_m$.

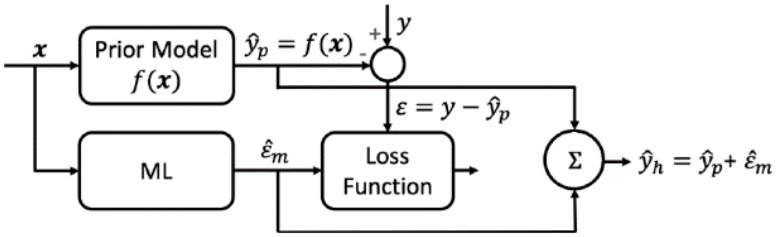

Figure. 3 DKIML Workflow

In the current study, new CHF LUT table similar to the Groeneveld 2006 version will be constructed. Therefore, the Groeneveld CHF LUT is selected as the domain knowledge, based on which ML models will be developed and trained. Same to the original LUT, the model input features are the system pressure (p), mass flux (G), flow channel hydraulic diameter (D_e), and local quality (x_e). And the model output is the CHF value. Both NN and RF methods will be used to develop CHF model. The performance of the final predicted output $\hat{y}_h$ is evaluated by its mean and standard deviation, as well as by the relative root-mean-square error (rRMSE):

$$rRMSE = \sqrt{\frac{1}{n}\sum_{i=1}^{n}\left(\frac{\hat{y}_h^i - y^i}{y^i}\right)^2} \quad (1)$$

where, n is the size of the dataset.

2.3. CHF Dataset

A collective CHF data set has been obtained and cleared for use from available literature both in upward tube [9-13] and upward annulus [14-16] flow geometry. The present data set represents a wide range of flow and heat transfer operating conditions which includes both the DO and DNB type CHF. **Table I** shows the ranges for each input parameters for tube and annulus data set. It can be seen that the current data sets cover the entire operating ranges that will be encountered in a nuclear system.

Table I. Input Space Ranges for Tube and Annulus

Tube	**Min**	**Max**
Pressure (kPa)	310	20000
Mass Flux (kg/m^2s)	241	7975
Hydraulic Diameter (m)	0.0011	0.0375
Quality (-)	-0.48536	1
Annulus	**Min**	**Max**
Pressure (kPa)	4088.6	15513
Mass Flux (kg/m^2s)	353.98	5913.2
Hydraulic Diameter (m)	0.004572	0.0127
Quality (-)	-0.14622	0.615

There are in total 1699 and 464 data points collected for the tube and annulus geometry, respectively. In order to evaluate the overall performance of the new CHF LUT constructed by the ML models, a 10% subset was retained for the final model testing for each tube and annulus data set. This subset is not used in the ML training process such that the ML models developed can be evaluated independently. On the other hand, the rest 90% subset is used in the training process.

To guarantee a fair evaluation of the ML models developed, the final testing subset sampled should be representative in terms of statistics for the overall dataset. Both tube and annulus data sets were randomly shuffled multiple times before sampling. **Figures 4** and **5** show the Groeneveld 2006 CHF LUT predictions for the two subsets for both tube and annulus geometry. Several insights can be drawn from the comparison. 1). Both the sampled 10% subsets for tube and annulus cover the same ranges of CHF values; 2). The 10% subsets have similar mean and standard deviation as the 90% subsets, indicating that it is a valid and representative dataset for final testing; 3). The Groeneveld 2006 CHF LUT can predict both the tube and annulus CHF values within 70% error span. However, due to its simple geometry, the prediction statistics for tube are found to be better compared with that of annulus. Also note that for the annulus geometry, the heated diameter, D_h, was used rather than the hydraulic diameter, D_e, in the LUT to achieve better performance.

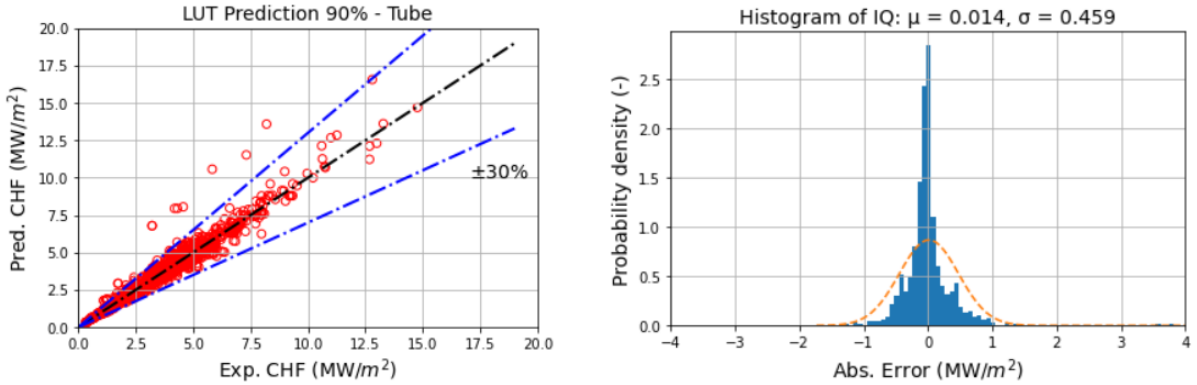

(a) ML Data Set (90%)

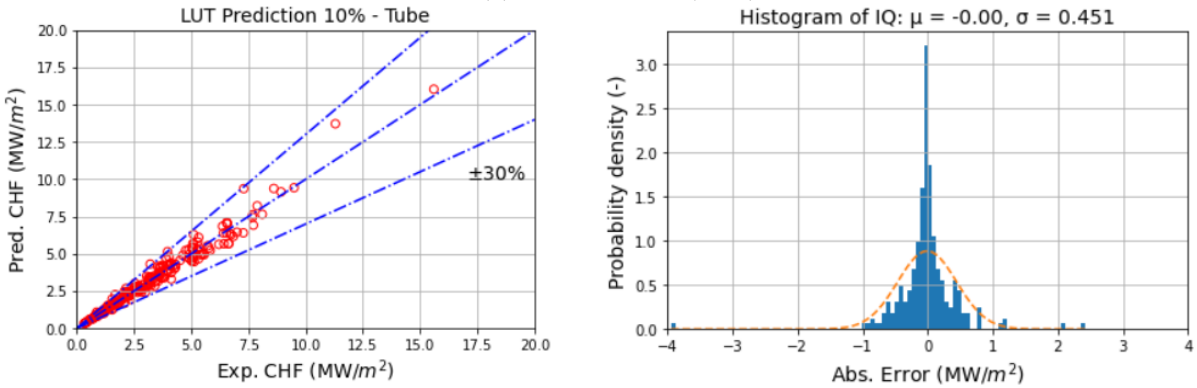

(b) Final Testing Data Set (10%)

Figure. 4 Groeneveld 2006 CHF LUT Prediction - Tube

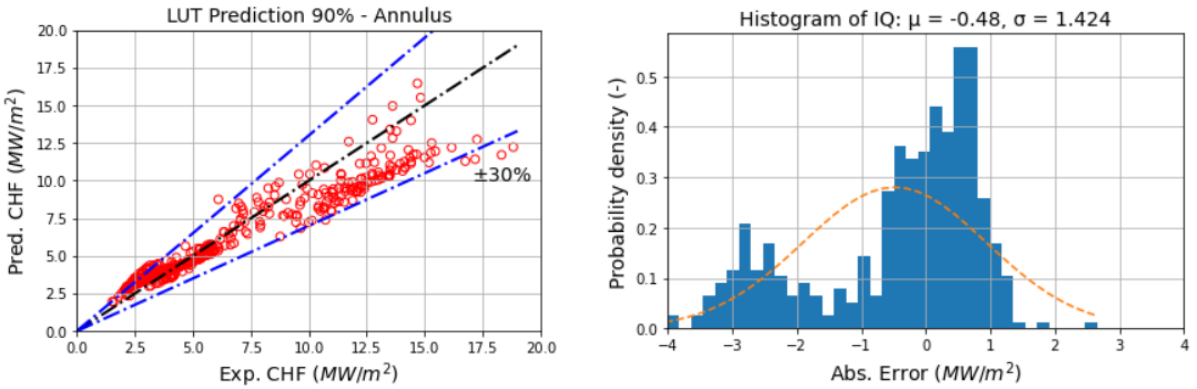

(a) ML Data Set (90%)

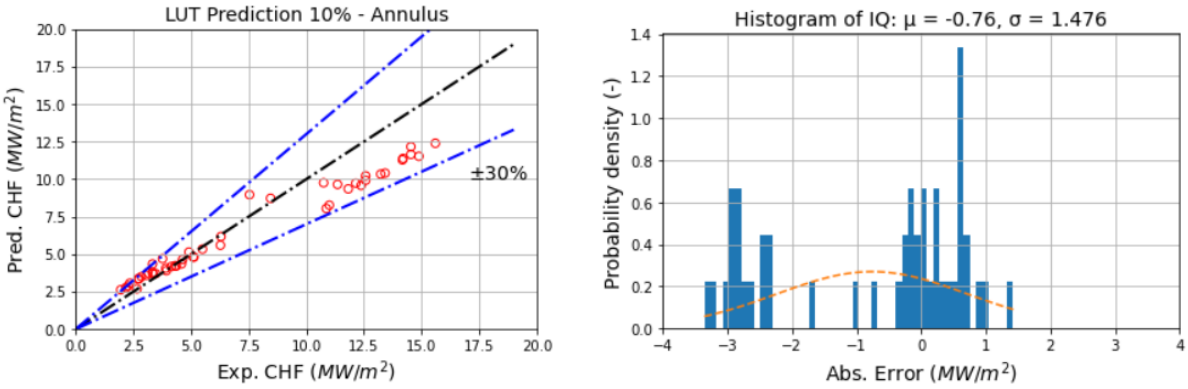

(b) Final Testing Data Set (10%)

Figure. 5 Groeneveld 2006 CHF LUT Prediction - Annulus

In the ML model training process, the 90% subset was further shuffled and divided into training set and validation set with ratio 9:1. Data in the training set will be seen and learned by the training process and will be used to obtain hyperparameters for the model. While data in the validation set will be used to evaluate the model performance and adjust these parameters accordingly at the end of each batch iteration.

3. RESULTS AND DISCUSSION

This section presents the LUT and ML model prediction results for the collected CHF dataset. The model architecture for RF is: 65 trees/estimators, 50%-70% features in each individual tree, no regularization. The model architecture for NN is: 4/32/64/32/1, Adam optimizer (learning rate = 0.001), "ReLU" activation, no regularization. An extensive grid search was also performed to determine the optimal epoch number and batch size (epoch = 250, batch size = 25 for tube and epoch = 150, batch size = 20 for annulus). In addition, to avoid the potential overfitting problem, both RF and NN are trained using 10-fold cross-validation technique.

1.1. Performance of Trained ML Models

Figures 6 and **7** show CHF prediction capabilities for tube and annulus during the training process by RF and NN using the 90% subset, respectively. At the end of training, the RF model obtained was able to significantly reduce the CHF prediction error for tube and annulus from 30% down to only 10%. The prediction mean and standard deviation were also reduced, especially for the annulus data prediction.

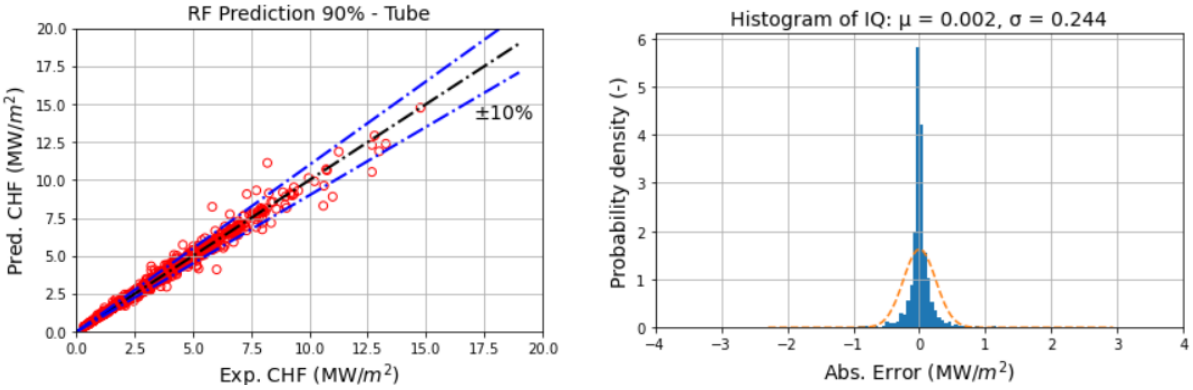

(a) ML Data Set (90%) - Tube

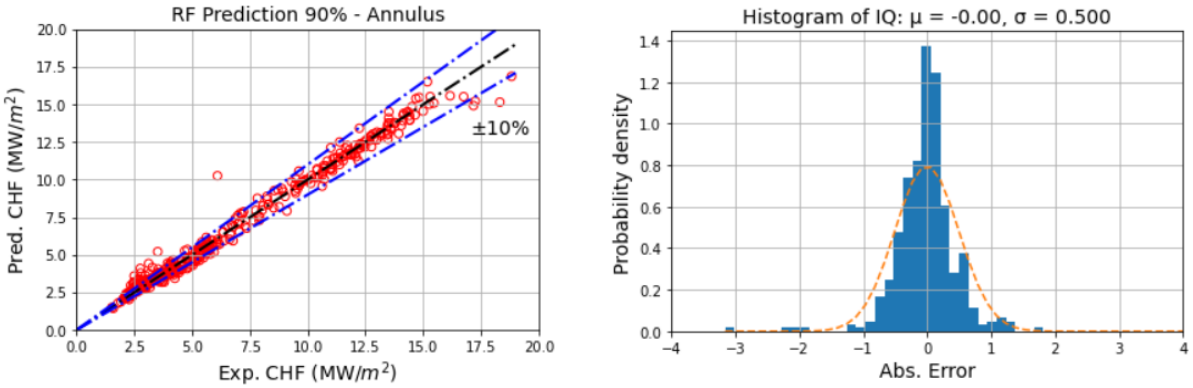

(b) ML Data Set (90%) - Annulus

Figure. 6 Trained RF ML Model CHF Prediction for 90% Subset

The developed NN model had very similar performance as the RF model, indicating that both ML methods can be effectively used in constructing the CHF model for nuclear applications. It has been proved in the study by Jin et al., 2021 [5] that the DKIML is able to not only solve the "black-box" problem existed in pure ML process but also generate robust final prediction results.

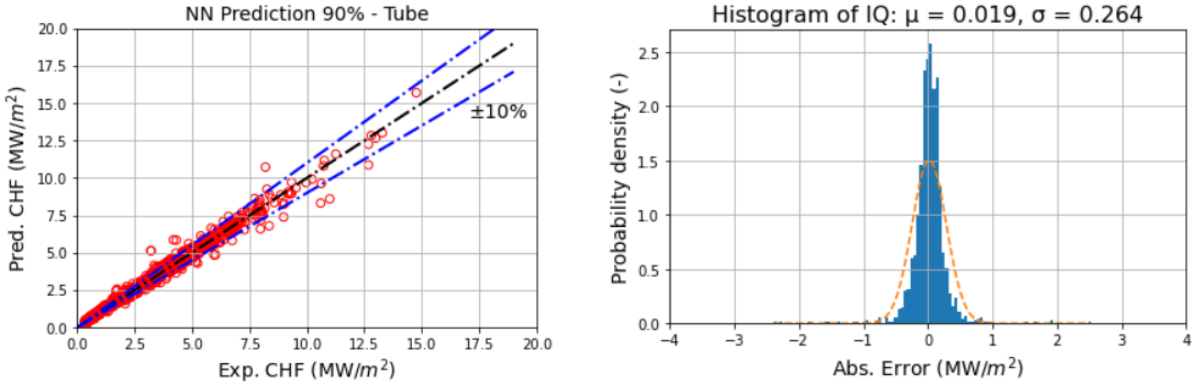

(a) ML Data Set (90%) - Tube

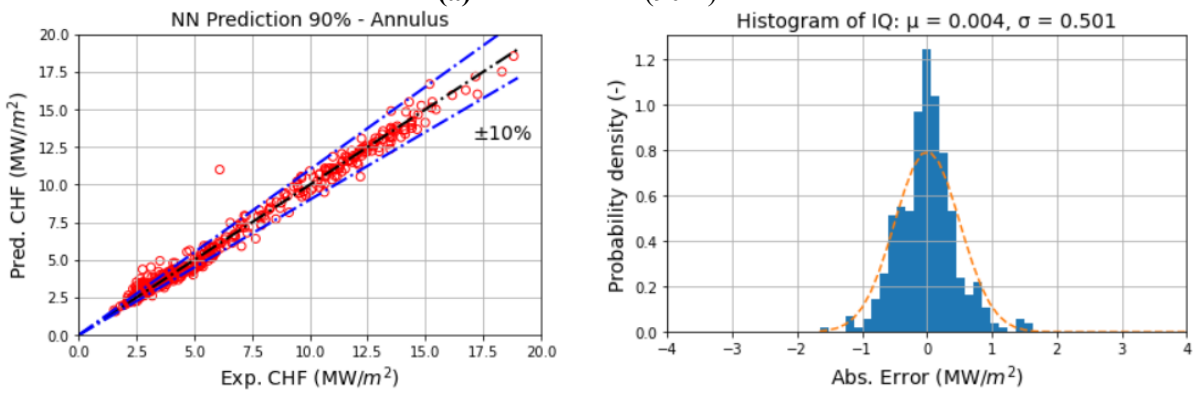

(b) ML Data Set (90%) - Annulus

Figure. 7 Trained NN ML Model CHF Prediction for 90% Subset

The trained RF and NN models are then tested by the 10% subset CHF data in order to make sure that they exhibit similar behavior when predicting unseen data. The testing results are shown in **Figure 8** for RF and **Figure 9** for NN, respectively. It can be seen from both figures that the ML models developed are indeed reliable in both cases with even better statistics due to smaller data set and less scatter. However,

the better statistics obtained for the annulus does not necessarily indicate that the ML models are better for annulus. This is partially due to the much less data was collected for the annulus than that of tube.

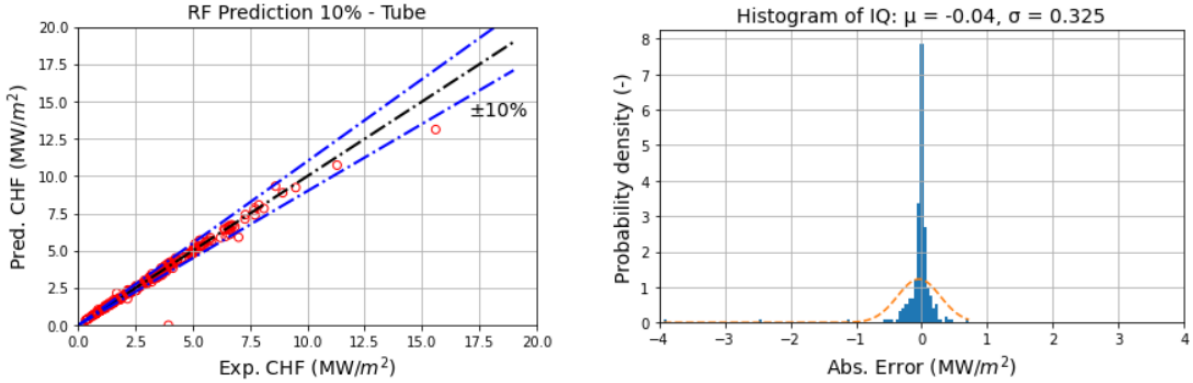

(a) Final Testing Data Set (10%) - Tube

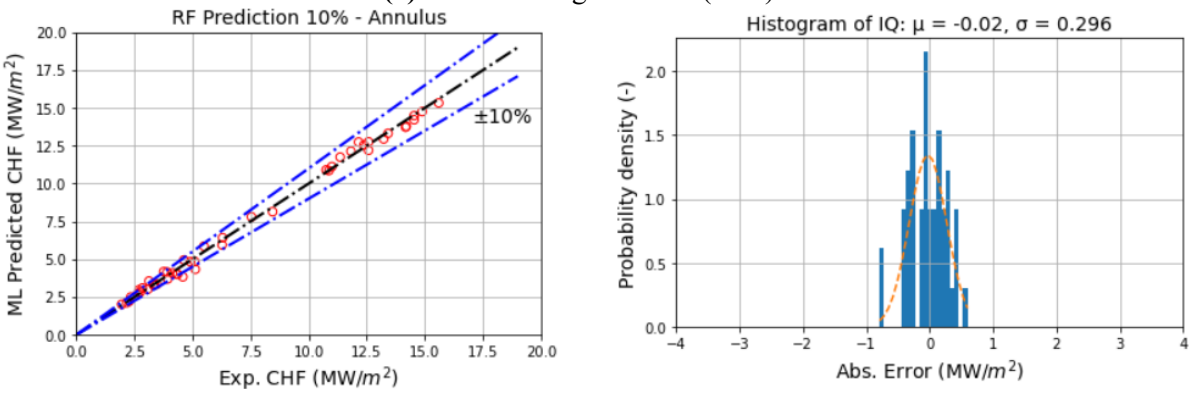

(b) Final Testing Data Set (10%) - Annulus

Figure. 8 Trained RF ML Model CHF Prediction for 10% Subset

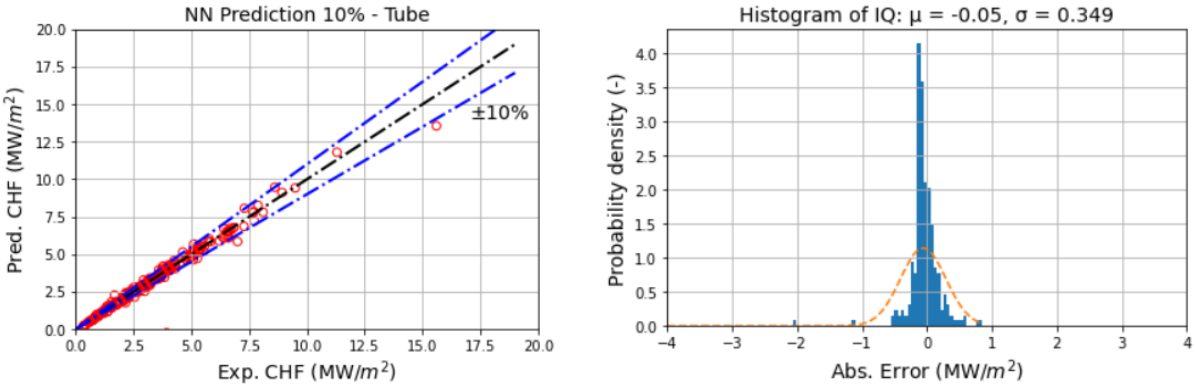

(a) Final Testing Data Set (10%) - Tube

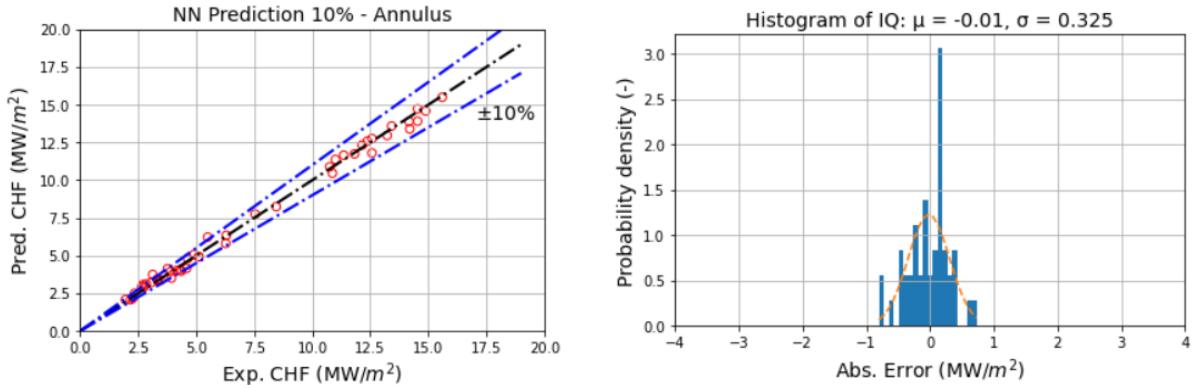

(b) Final Testing Data Set (10%) - Annulus

Figure. 9 Trained NN ML Model CHF Prediction for10% Subset

1.2. Performance of the New ML LUT Models

The comparisons made in the previous section shows the superior capabilities of the DKIML models as compared to the pure Groeneveld LUT. But it's usually difficult to apply such trained models in actual practices such as incorporating them into numerical analysis tools. As a result, it is desired to construct a new CHF LUT based on the ML predictions with simple structure but with improved accuracy and reduced scatter. The same interpolation scheme of the Groeneveld 2006 CHF LUT was used in the present construction process of new tables and the new table application range can be found in **Table I**.

Figure 10 first shows RF LUT performance evaluated by the 10% testing subset. Compared with the direct RF model prediction in **Figure 11**, it is observed that the new RF LUT has slightly larger error and standard deviation. This is the expected behavior due to the linear interpolation method used. However, when it is compared with the Groeneveld 2006 CHF LUT prediction of 10% subset in **Figures 4** and **5**, significant improvement in model performance can be obtained, indicating that constructing a new LUT using ML is effective.

Very similar trends were obtained for the NN LUT as well, as is shown in **Figure 11**. For both tube and annulus, the CHF values can be well captured within 10% error, improving the original LUT capability and as the same time eliminating the performance inconsistence in tube and annulus prediction.

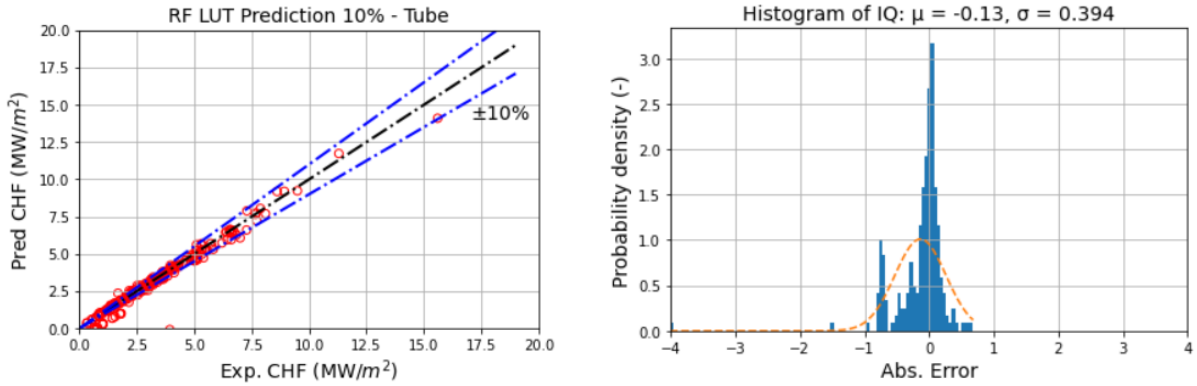

(a) Final Testing Data Set (10%) - Tube

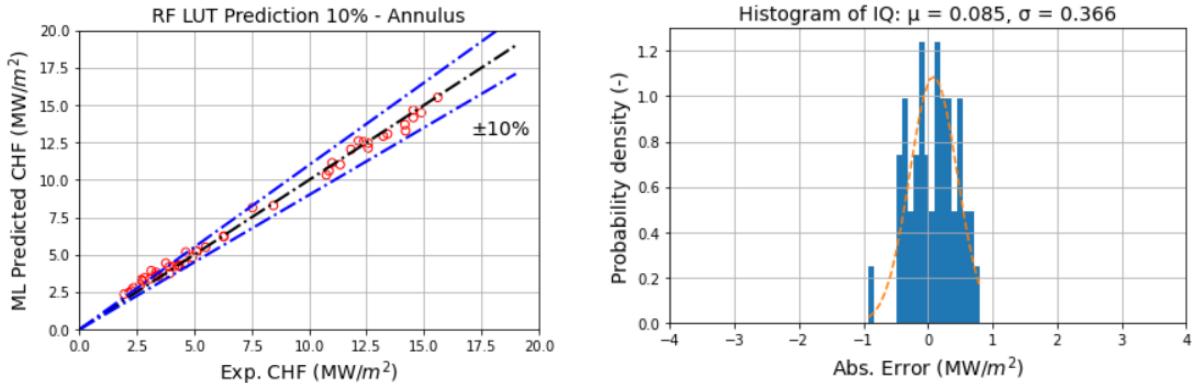

(b) Final Testing Data Set (10%) - Annulus

Figure. 10 Constructed RF ML LUT Prediction for10% Subset

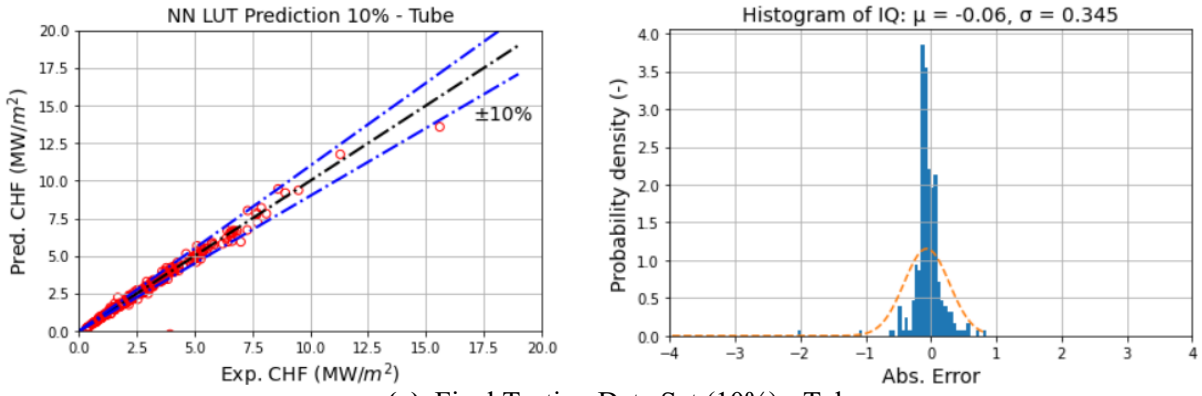

(a) Final Testing Data Set (10%) - Tube

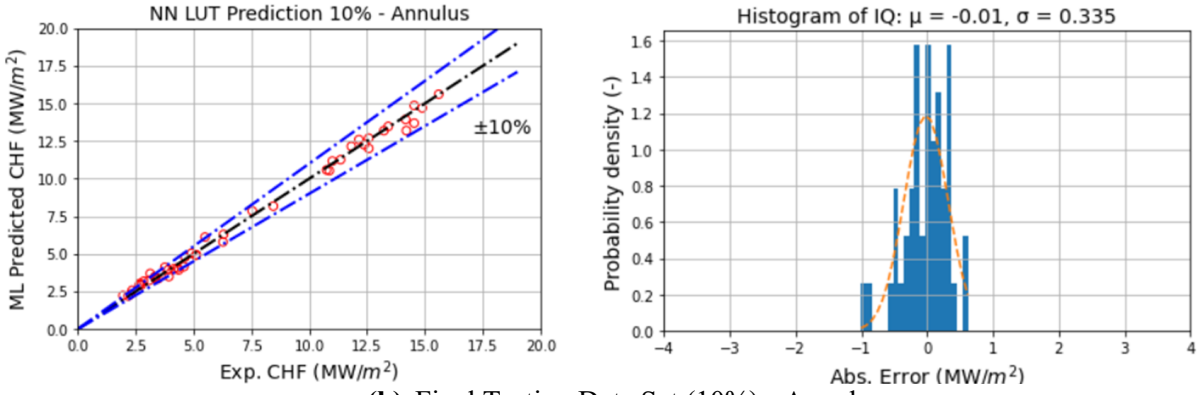

(b) Final Testing Data Set (10%) - Annulus

Figure. 10 Constructed NN ML LUT Prediction for10% Subset

A summary of the new ML model performance is summarized in **Table II** for tube and **Table III** for annulus. The rRMSE values are also included. It can be seen that, no significant improvement can be achieved for the tube geometry as compared with the conventional Groeneveld CHF LUT due to the fact that the old LUT was originally constructed for tube geometry. However, significantly improvement is observed for the annulus CHF prediction. Both the prediction mean, standard deviation as well as the rRMSE were reduced by through applying of the ML technology.

Table II. Summary of the ML Model Prediction for 10% Final Testing Subset - Tube

Tube	CHF LUT 2006	ML Direct Prediction		New ML LUT	
		RF	NN	RF	NN
Mean (μ)	0.00	-0.04	-0.05	-0.13	-0.06
Std. (σ)	0.451	0.325	0.349	0.394	0.345
rRMSE	0.110	0.077	0.113	0.350	0.111

Table III. Summary of the ML Model Prediction for 10% Final Testing Subset - Annulus

Annulus	CHF LUT 2006	ML Direct Prediction		New ML LUT	
		RF	NN	RF	NN
Mean (μ)	-0.76	-0.02	-0.01	0.085	-0.01
Std. (σ)	1.476	0.297	0.325	0.366	0.335
rRMSE	0.181	0.057	0.063	0.099	0.065

3. CONCLUSIONS

In this study, motivated by the idea of constructing a new CHF LUT based on the advanced ML techniques with improved accuracy and reliability, extensive efforts were focused on the development of the domain knowledge informed machine learning models using RF and NN methods. The models were developed for the various vertical flow conditions within tube and annulus geometry. An extensive experimental CHF data were collected in the current study for both DNB and DO type CHF, which was used to train and validate the ML models with the Groeneveld 2006 look-up table being the domain knowledge. The key input parameters used include system pressure, mass flux, channel hydraulic diameter as well as the local fluid quality.

Base on the results obtained for the final testing subset, it was found that the new ML look-up table shows improved accuracy for conditions relevant to PWRs and BWRs. The RF and NN models typically have similar performance. In addition, its domain knowledge informed nature ensures that a rationale prediction can be made, thus accounting for the underling physics in the machine learning model training process. The new ML LUT has exactly the same structure and interpolation scheme as the Groeneveld 2006 LUT. It can be easily applied into practical use or in various numerical analysis tools to achieve superior performance. In the future, thorough evaluation will be performed to investigate the uncertainty and sensitivity of the new LUT in terms of input data and the new LUT will be used in actual nuclear power plant safety analysis.

REFERENCES

1. . N. E. Todreas and M. S. Kazimi, Nuclear Systems. Volume I: Thermal Hydraulic Fundamentals, 2nd ed. Boca Raton: CRC Press (2012).
2. D. C. Groeneveld et al., “The 2006 CHF Look-Up Table,” Nucl. Eng. Des., 237, 1,909–1,922 (2007).
3. X. Zhao et al., “Critical Power and Void Fraction Prediction of Tight Bundle Designs,” Nucl. Tech., 196, 3, 553–567 (2016).
4. Kim et al., Prediction of critical heat flux for narrow rectangular channels in a steady state condition using machine learning, Nuclear Engineering and Technology, Volume 53, Issue 6, (2021), Pages 1796-1809.
5. Y. Jin, X.G. Zhao, and K. Shirvan. Unified Domain Knowledge Informed Machine Learning Model for CHF Prediction. 2021 ANS Virtual Annual Meeting, Jun. 14-16, 2021.

6. X. Zhao et al., “On the Prediction of Critical Heat Flux Using a Physics-Informed Machine Learning Aided Framework,” Appl. Thermal Eng., 164, 114540 (2020)
7. Hae Min Park, Jong Hyuk Lee, Kyung Doo Kim, Wall temperature prediction at critical heat flux using a machine learning model, Annals of Nuclear Energy, Volume 141, 2020, 107334, ISSN 0306-4549.
8. M.F. He, Y. Lee, Application of machine learning for prediction of critical heat flux: Support vector machine for data-driven CHF look-up table construction based on sparingly distributed training data points, Nuclear Engineering and Design, Volume 338, 2018, Pages 189-198, ISSN 0029-5493.
9. F. Inasaka, H. Nariai, Critical heat flux of subcooled flow boiling for water in uniformly heated straight tubes, Fusion Eng. Des. 19 (1992) 329–337. doi:10.1016/0920-3796(92)90007-Q.
10. O.L. Peskov, V.I. Subbotin, B.A. Zenkevich, N.D. Sergeyev, The critical heat flux for the flow of steam-water mixtures through pipes, Probl. Heat Transf. Hydraul. Two Phase Media. (1969) 48–62.
11. B. Thompson, R.V. Macbeth, Boiling water heat transfer burnout in uniformly heated round tubes: a compilation of world data with accurate correlations. United Kingdom Atomic Energy Authority Report AEEW-R356, 1964.
12. R.J. Weatherhead, Nucleate boiling characteristics and the critical heat flux occurrence in subcooled axial-flow water systems. Argonne National Laboratory Report ANL-6675, 1963. doi:10.2172/4727562.
13. C.L. Williams, S.G. Beus, Critical heat flux experiments in a circular tube with heavy water and light water. AWBA Development Program, WAPD-TM-1462, 1980.
14. S.G. Beus, O.P. Seebold, Critical heat flux experiments in an internally heated annulus with a non-uniform, alternate high and low axial heat flux distribution. AWBA Development Program, WAPD-TM-1475, 1981. doi:10.2172/6655346.
15. E. Janssen, J.A. Kervinen, Burnout conditions for single rod in annular geometry, Water at 600 to 1400 psia. GEAP-3899, 1963. doi:10.2172/4136515.
16. E.P. Mortimore, S.G. Beus, Critical heat flux experiments with a local hot patch in an internally heated annulus. LWBR development program, WAPD-TM-1419, 1979.

APPENDIX A

The constructed ML CHF look-up table can be found at: https://github.com/doubtperfect/ML_CHF_LUT.